

CORE MATHEMATICS TO SUPPORT NEW THEORY FOR DISTRIBUTIONS OF
BIOLOGICAL DIVERSITY ALONG ENVIRONMENTAL GRADIENTS

NCSU Dept. of Statistics Technical Report

June 18, 2015

Kevin Gross and Andrew Snyder-Beattie

Biomathematics Program
North Carolina State University
CB 8203
Raleigh, NC 27695

1 Abstract

Latitudinal and elevational biodiversity gradients have inspired dozens of hypotheses to explain their existence. Among these, some have suggested that the geometry of environmental variation may promote species-richness gradients, although a mathematical model has yet to appear that fully captures this hypothesis. In this technical report, we provide the mathematical results that support a new “environmental geometry” model that fills this gap. The model characterizes species ranges by a maximal range extent and by species’ environmental niches, and places those ranges onto the simplified environmental geometries of a sphere or cone. The model generates surprising and nuanced predictions for species-richness gradients, including low-latitude (but non-Equatorial) maxima and mid-latitude inflection points in latitudinal diversity gradients, and low-elevation maxima in elevational diversity gradients. These results suggest that environmental geometry may play a deeper role in driving biodiversity gradients than previously appreciated.

2 Introduction and background

The latitudinal gradient in biological diversity is one of the most pervasive, conspicuous, and ancient characteristics of life on Earth (Crame, 2001; Hillebrand, 2004). Decades of research have identified over 30 potential mechanisms for Earth’s latitudinal diversity gradient (LDG) (Lomolino *et al.*, 2010; Brown, 2014), including ecological (reviewed in e.g. Willig *et al.*, 2003), evolutionary (e.g. Jablonski *et al.*, 2006) and historical (reviewed in Mittelbach *et al.*, 2007) explanations. While a myriad of interacting mechanisms likely contribute to Earth’s LDG (Colwell, 2011), scientific debate about the merits and relative importance of these proposed mechanisms continues with vigor.

In recent decades, a line of argument has emerged that suggests that biodiversity gradients (including Earth’s LDG) may arise in part because of geometric constraints on the placements of species ranges (Colwell & Hurtt, 1994; Willig & Lyons, 1998; Lees *et al.*, 1999; Colwell & Lees, 2000). This hypothesis suggests that when species ranges are placed randomly within a bounded territory, the overlap of species ranges will be greatest near the center of the territory, and will decline towards the boundaries of the territory. If species diversity is determined by (or at least positively correlated with) the overlap of species ranges, then biological diversity will have a similar mid-domain peak. Such a phenomenon has been called the mid-domain effect (MDE; Colwell & Lees (2000)). The first mathematical descriptions of the MDE involved linear species ranges placed along

30 a linear territory (Colwell & Hurtt, 1994; Lees *et al.*, 1999), and more recent work has explored the
placement of two-dimensional ranges on flat, two-dimensional territories (e.g. Jetz & Rahbek, 2001;
32 Davies *et al.*, 2007; Rangel *et al.*, 2007; Colwell *et al.*, 2009). Most geometric constraint models have
(often intentionally) ignored environmental gradients within the domain. Two notable exceptions
34 are Connolly (2005), who investigated a linear territory with an environment that was symmetric
about its midpoint, and Rangel & Diniz-Filho (2005), who studied a linear domain with a monotonic
36 gradient in environmental suitability. Both studies showed that environmental variation can modify
the predictions of MDE models depending on the strength of the environmental gradient, although
38 both still predicted that species richness would peak within the interior of the domain.

While Connolly (2005) and Rangel & Diniz-Filho (2005) offer tantalizing suggestions that envi-
40 ronmental variation can modify the predictions of range-overlap models in interesting ways, neither
model adequately captures the geometry of environments on Earth, to the extent that environment
42 is determined by latitude. Indeed, many ecologists (most notably Terborgh (1973) and Rosenzweig
(1995)) have stressed the importance of Earth’s geometry for driving the LDG. Tropical environ-
44 ments occupy a greater contiguous area than any other ecoregion on Earth, for three reasons. First,
parallels of latitude have the greatest circumference at the Equator, and become shorter as one ap-
46 proaches the poles. Second, the tropical regions of the Northern and Southern hemisphere form one
contiguous climate belt, while temperate and polar regions of the Northern and Southern hemi-
48 sphere are disjunct. Third, as Terborgh (1973) first observed, the latitudinal temperature gradient
is non-linear, in the sense that the rate of change of temperature with respect to latitude becomes
50 steeper as one moves from low to high latitudes. Terborgh (1973) and Rosenzweig (1995) (among
others) have suggested that the greater contiguous area of the tropics is a major driver of Earth’s
52 LDG, because larger area leads to larger population sizes, which in turn promote speciation rates
and reduce extinction rates.

54 In this contribution, we describe the first model (of which we know) for biodiversity that fully
accommodates environmental gradients on the surface of an Earth-like sphere. The model assumes
56 that species ranges are limited by dispersal (and thus have a maximal radius) and by fidelity
to an environmental niche, and follows other range-overlap models in equating species diversity
58 with the overlap of species ranges. We dub our model the “environmental geometry” model. As
we will see, the model illuminates how Earth’s latitudinal environmental gradient can drive a
60 LDG, and generates testable and surprising predictions about the shape of such gradients. The
model can in fact be applied more generally than to just a sphere, although the mathematical

62 details differ depending on the geometry considered. We also use the model to explore elevational
diversity gradients (EDGs) on mountainsides by applying the model to a cone. Admittedly, many
64 mountains (especially those created by tectonic uplift) have complicated shapes, but we suggest
that the simplified geometry of a cone is a useful starting point for investigating EDGs.

66 This model advances our understanding of how dispersal limitation and environmental niche
fidelity can drive biodiversity along environmental gradients in two important ways. First, linear
68 geometries are simply unable to capture the full geometric implications of latitudinal and elevational
environmental gradients. As we will show, these geometries generate predictions that have not
70 been available on linear territories. Secondly, by modeling environmental gradients on a sphere,
the model eliminates the need to impose a boundary on the habitable territory. The MDE relies
72 crucially on the existence of a boundary (Colwell & Hurtt, 1994). While some territorial boundaries
are incontrovertible (e.g., land / sea interfaces), the need to invoke a boundary for Earth’s LDG
74 is unsatisfying. Colwell & Hurtt (1994) originally took their boundaries to be the “northern and
southern limits of habitable latitudes ... for a particular group of organisms”. While many taxa
76 do indeed have northern and southern range limits (that is, are limited to latitudes *below* a certain
threshold), restricting the model to species whose ranges are limited thusly inherently restricts the
78 model to taxa with non-polar niches. How might we account for taxa with polar niches, that is, taxa
whose ranges are limited to latitudes *above* a certain threshold? To be clear, we do not question
80 the logic behind the MDE on genuinely bounded territories, nor do we dispute that most known
taxa have physiologies that restrict their ranges to below a certain latitude. However, the MDE’s
82 implicit restriction to non-polar taxa leaves it wanting as an explanation for the LDG. With the
model below, we show that the geometry of Earth’s latitudinal environmental gradient can generate
84 an LDG even when all environments are equally suitable for life.

The rest of this report describes the mathematical foundations of our model. We discuss linear,
86 conical and spherical territories; the former two are interesting both in their own right, and for
developing intuition about the results on the sphere. The beginnings of this theory were described
88 in Andrew Snyder-Beattie’s 2013 MS thesis (Snyder-Beattie, 2013). The ecological consequences
of our model will be explored more fully in future work.

90 **3 Basic notation**

Let \mathcal{A} represent a geometry (e.g., line segment or surface). Generically, let $a, b \in \mathcal{A}$ be two points
92 on that geometry. Let $g : \mathcal{A} \mapsto [0, 1]$ define the environment at each point in \mathcal{A} . Throughout,

g will depend on only one dimension of \mathcal{A} , regardless of the actual dimensionality of \mathcal{A} . Let
94 $d(a, b) : \mathcal{A} \times \mathcal{A} \mapsto \mathcal{R}^+$ define the distance between any two points in \mathcal{A} . Loosely, $d(a, b)$ is the
shortest path between a and b that does not leave \mathcal{A} . (So, for example, if \mathcal{A} is the surface of a
96 sphere, then $d(a, b)$ is the great-circle distance between any two points on that surface. It is not
the distance given by connecting a and b through the interior of the sphere.) Finally, we let x
98 generically denote the position along a transect of interest on \mathcal{A} .

The following geometries and coordinate systems are considered:

100 **The line.** The line segment is a useful context for developing ideas. We consider the unit interval
 $x \in [0, 1]$ for a constant or unidirectional gradient, or the interval $x \in [-1, 1]$ for an internally
102 reflected gradient. The distance is the obvious $d(x, y) = |x - y|$.

The surface of a cone. The cone is the basic geometry for EDGs on mountainsides. The coor-
104 dinates for a cone are $(x, \phi) \in [0, 1] \times [-\pi, +\pi]$, where x is the position along a base-to-peak
transect on the cone’s surface, with $x = 0$ corresponding to the base and $x = 1$ corresponding
106 to the peak. The coordinate ϕ is the compass direction with respect to “east”. The envi-
ronment $g(\cdot)$ depends only on x . Let $\alpha \in (0, \pi/2]$ be the opening angle of the cone, such
108 that $\alpha = 0$ corresponds to an infinitely steep cone and $\alpha = \pi/2$ corresponds to a disc. Let
 $h = \cos \alpha$ be the height of the cone, and $r = \sin \alpha$ be the radius of the cone’s base. As we will
110 see, α is only relevant for EDGs under some circumstances. The cone / disc is also a useful
geometry for contemplating LDGs at high latitudes, as a pole is topologically similar to the
112 peak of the cone (or center of the disc).

With cones or discs, we can distinguish between “isolated” and “embedded” cones, where
114 isolated cones are those where the edge forms a hard boundary for life, and embedded cones
are those where the base sits on a surrounding landscape that has the same environment as
the cone’s base. Loosely, we might think of isolated and embedded cones as reasonable first
116 models for oceanic and terrestrial mountains, respectively. In this report, we only consider
isolated cones and discs. We do so because results on the embedded cone or disc are sensitive
118 to the assumptions that one makes about the properties of the species on the embedding
landscape. Thus, while we comment qualitatively on the differences that one would expect
120 between isolated vs. embedded cones, we avoid a quantitative study.

122 For isolated cones and discs, $d(\cdot, \cdot)$ is equal to the Euclidean distance on the unwrapped cone.

The surface of a sphere. The surface of a sphere is the basic geometry for LDGs. The coordinate

124 system is $(x, \phi) \in [-\pi/2, +\pi/2] \times [-\pi, +\pi]$. The first coordinate, x , is the latitude. The second
coordinate, ϕ , is the longitude. The environment $g(\cdot)$ depends only on latitude. The distance
126 $d(\cdot)$ is a great-circle distance.

We will also consider cones with uninhabitable zones at their tops, and spheres with uninhab-
128 itable ice caps at their poles. When there is an uninhabitable region, we use \tilde{x} to denote the
boundary of that region. For a cone or disc, the habitable region will be $x \in [0, \tilde{x}]$. For the surface
130 of a sphere, the habitable region is $x \in [-\tilde{x}, \tilde{x}]$.

The environment satisfies the following properties:

- 132 • (E1). The environment $g(\cdot)$ depends only on a single coordinate (namely, x), and thus can
be written as $g(x)$.
- 134 • (E2). If $x < 0$ is allowed, then the environment is symmetric, i.e., $g(-x) = g(x)$.
- (E3). The environment is monotonic with respect to $|x|$.

136 We will also often require the stronger condition:

- (E4). The environment is strictly monotonic with respect to $|x|$.

138 Conditions (E1)–(E4) allow us to define the (non-negative) inverse as $g^{-1} : [0, 1] \mapsto [0, x_{\max}]$,
where x_{\max} is the maximum value of x , and g^{-1} always maps to the non-negative values of x .
140 Finally, although it is not critical, without loss of generality we will assume

- (E5). The environment is strictly increasing across $x > 0$, with $g(0) = 0$ and $g(x_{\max}) = 1$.

142 The only environments we will consider that do not satisfy (E4)–(E5) are constant environments.
All other environments satisfy (E1)–(E5).

144 We will work with the following environments:

- On the line:
 - 146 – A constant environment: $g(x) = c$, where $x \in [0, 1]$, and c is some constant in $[0, 1]$.
 - A unidirectional environment: $g(x) = x$, where $x \in [0, 1]$.
 - 148 – A reflected environment: $g(x) = |x|$, where $x \in [-1, 1]$.

- On the disc / cone:

150 – A linear environment: $g(x) = x$ for $x \in [0, 1]$.

• On the surface of a sphere:

152 – A cosine environment: $g(x) = 1 - \cos x$. (We use $1 - \cos x$ so that $g(x)$ is an increasing function of x .)

154 – A (reflected) linear environment: $g(x) = |2x/\pi|$. This environment does not have a biological interpretation, but is useful for understanding the relationship between the
156 line, cone and sphere geometries.

Species ranges are constructed on the basis of three characteristics. They are:

158 • Each range has an **origin**, denoted as $a_o \in \mathcal{A}$. A species' optimal environment is simply the environment at its range origin, i.e., $g(a_o)$.

160 • Each range is limited by an **environmental tolerance**, denoted as $\gamma \in [0, 1]$. A range originating at a_o will be a subset of the locations $\{b : |g(b) - g(a_o)| \leq \gamma\}$. Species with larger
162 γ can tolerate a broader range of environments.

• Each range has a **distance limit**, denoted as $\delta \geq 0$. A species range can extend at most a
164 distance δ from the range origin. That is, given an origin a_o , a species range will be a subset of points b where $d(a_o, b) \leq \delta$.

166 The triple (a_o, γ, δ) fully defines the characteristics of a species. Given these characteristics, we can define a species range in the following way. Let

$$\mathcal{E} = \{b : |g(b) - g(a_o)| \leq \gamma\}$$

168 denote the collection of points that fall within a species' environmental tolerance, and let

$$\mathcal{D} = \{b : d(a_o, b) \leq \delta\}$$

denote the collection of points that fall within a species' distance limit. One possible definition
170 of a species' range is the intersection $\mathcal{E} \cap \mathcal{D}$. However, this definition allows for non-contiguous ranges. An easy way to see this is to consider the reflected linear environment on $[-1, 1]$, and to
172 consider a range originating at (say) $x_o = 0.5$, with a small environmental tolerance (say, $\gamma = 0.1$) and a large distance limitation (say, $\delta = 2$). For this species, $\mathcal{E} \cap \mathcal{D} = [-.6, -.4] \cup [.4, .6]$, that
174 is, two blocks of allowable habitat separated by a large swath of uninhabitable territory. We do

not allow such a range. (One biological justification for insisting that ranges must be contiguous
176 is that a species with a non-contiguous range is likely to evolve into multiple separate species over
evolutionary time.)

178 In our model, we define a species range as (D1): the contiguous subset of $\mathcal{E} \cap \mathcal{D}$ that contains
the range origin, a_o . In the example above, the species' range would thus be $[.4, .6]$. Put another
180 way, the range consists of all points in \mathcal{D} that are connected to a_o by a path that lies entirely in \mathcal{E} .

For one-dimensional geometries (i.e., the line), the definition (D1) is the only reasonable option.
182 For two-dimensional geometries, a second definition is viable. The essential distinction is that, in a
two-dimensional geometry and under (D1), the distance constraint is enforced "as the crow flies",
184 without regard to whether or not the habitat along the crow's path lies within \mathcal{E} . Thus, the shortest
path between a point in a species range and the range origin that passes through only \mathcal{E} may have
186 length $> \delta$. Thus, on two-dimensional geometries, we could also define a species range as (D2): the
contiguous subset of $\mathcal{E} \cap \mathcal{D}$ that contains the range origin, a_o , and for which any point in the range
188 is connected to the range origin a_o by a path that is no longer than δ and lies entirely within \mathcal{E} .
In what follows, we use (D1). (D2) would seem to have a stronger biological justification, but the
190 math is considerably more tractable with (D1). (In fact, the math with (D2) is likely to be very
hard, and thus results will likely only be available with simulation.)

192 Next, we place a probability distribution on the triple (a_o, γ, δ) . For simplicity, we assume
that these three characteristics are independent, though this assumption could be relaxed if two or
194 more of the characteristics were thought to be correlated. Generically, let $f(\cdot)$ denote a probability
density, so that $f(a_o)$, $f(\gamma)$ and $f(\delta)$ are the probability densities associated with each of the three
196 characteristics. For example, if we want to assume that range origins are uniformly distributed, the
corresponding densities are $f(x) = 1$ or $= 1/2$ for lines on $[0, 1]$ or $[-1, 1]$, respectively; $f(x, \phi) =$
198 $(1/4\pi)^{-1} \cos x$ for the sphere, and $f(x, \phi) = (1 - x)/(\pi \sin \alpha)$ for the cone or disc.

Let $S(a)$ denote the species richness at any point $a \in \mathcal{A}$. Simply, $S(a)$ is the fraction of species
200 ranges that overlap the point a . Throughout, if we are interested in how species richness varies
across a transect indexed by x , we will write that richness as $S(x)$.

202 Finally, we make one additional observation that will prove useful later. We say that an envi-
ronment *communicates* if, for all $a, b \in \mathcal{A}$, and for a given choice of γ and δ , a range originating
204 at a includes b if and only if a range originating at b includes a . We conjecture that, under defi-
nition (D1) for species ranges, a necessary and sufficient condition for communication is that, for
206 all $a, b \in \mathcal{A}$, there exists a path (of arbitrary distance) that connects a and b that passes only

through habitat whose environment is intermediate between $g(a)$ and $g(b)$; that is, $\forall x$ on the path,
 208 $g(a) \leq g(x) \leq g(b)$ (if, without loss of generality, $g(a) \leq g(b)$). It is clear that the above condition
 is sufficient for communication under (D1), although the necessity is less clear. Examples of en-
 210 vironments that communicate under (D1) are the line segment with a unidirectional environment,
 and a disc / cone with a linear environment. Examples of environments that do not communicate
 212 under (D1) are the line with the internally reflected environment, and the Equatorial regions of the
 surface of a sphere. Communication is much harder under (D2), and indeed may only be available
 214 for trivial environments (such as a constant environment).

Communication is important for the following reason. Usually, we will find the species richness
 216 at a location x by integrating the density of range origins over the region of origins for ranges that
 will include x . However, in a communicating environment, this region of integration is identical to
 218 the range originating at x . Thus, we can equivalently find the species richness at x by integrating
 the density of range origins over the area of a single range originating at x . This equivalence does
 220 not hold in non-communicating environments.

We are now ready to begin deriving results.

222 4 Results for the line

A line segment is a simple geometry that allows us to develop intuition. We will consider a line
 224 segment with a constant environment (to establish a baseline), a line segment with a unidirectional
 environment (a communicating environment), and a line segment with an internally reflected en-
 226 vironment (a non-communicating environment). The line segment with an internally reflected
 environment is a useful first model for a pole-to-pole transect running along a meridian of longi-
 228 tude, although we will ultimately show that the two-dimensional surface of a sphere is a more useful
 geometry for latitudinal richness gradients.

230 First consider the simple case of a line running from $x = 0$ to $x = 1$ with a strictly monotonic
 environment that satisfies (E1) – (E5). Let $S(x; \gamma, \delta)$ give the species richness at x if all species
 232 have environmental tolerance γ and distance limitation δ . $S(x; \gamma, \delta)$ is given by the integral

$$S(x; \gamma, \delta) = \int_{L(x)}^{U(x)} f(y) dy \quad (1)$$

where $f(\cdot)$ is the density of range origins, and $L(x)$ and $U(x)$ are the locations closest to 0 and 1,
 234 respectively, for which a range originating at that location would overlap x . Because the environ-
 ment communicates on $[0, 1]$, $L(x)$ and $U(x)$ can also be interpreted as the endpoints of the range

236 originating at x .

To find $L(x)$ and $U(x)$, consider a range originating at $y \in [0, 1]$, with distance limit δ and
 238 environmental tolerance γ . This species will have a range that overlaps x if and only if both of the
 following conditions are true. First, $d(x, y) = |x - y| \leq \delta$, that is,

$$(x - \delta) \vee 0 \leq y \leq (x + \delta) \wedge 1.$$

240 For consistency with later results, we re-write the above using x_{\max} instead of 1 for the maximum
 value of x , that is,

$$(x - \delta) \vee 0 \leq y \leq (x + \delta) \wedge x_{\max}.$$

242 Second, the environment at x must fall within the species environmental tolerance, that is,

$$(g(x) - \gamma) \vee 0 \leq g(y) \leq (g(x) + \gamma) \wedge 1$$

or

$$g^{-1}((g(x) - \gamma) \vee 0) \leq y \leq g^{-1}((g(x) + \gamma) \wedge 1).$$

244 Combining the distance and environmental constraints yields

$$\{(x - \delta) \vee 0\} \vee g^{-1}((g(x) - \gamma) \vee 0) \leq y \leq \{(x + \delta) \wedge x_{\max}\} \wedge g^{-1}((g(x) + \gamma) \wedge 1).$$

Because $g^{-1}(0) = 0$ and $g^{-1}(1) = x_{\max}$, the above can be written more simply as

$$(x - \delta) \vee g^{-1}((g(x) - \gamma) \vee 0) \leq y \leq (x + \delta) \wedge g^{-1}((g(x) + \gamma) \wedge 1).$$

246 Thus, we have the following formula for $L(x)$ and $U(x)$:

$$\begin{aligned} L(x) &= (x - \delta) \vee g^{-1}((g(x) - \gamma) \vee 0) \\ U(x) &= (x + \delta) \wedge g^{-1}((g(x) + \gamma) \wedge 1). \end{aligned} \tag{2}$$

Fig. 1a shows how species richness varies if the environment is constant, all species have distance
 248 constraint $\delta = 1/3$, and range origins are uniformly distributed ($f(x) = 1$). (Note that when the
 environment is constant, the environmental constraint γ is irrelevant. Note also that g^{-1} does not
 250 exist with a constant environment, although it can be easily shown in this case that $L(x) = (x - \delta) \vee 0$
 and $U(x) = (x + \delta) \wedge 1$.) Fig. 1c shows results for a smoothly varying environment, $g(x) = x$, when
 252 $\gamma = \delta = 1/3$.

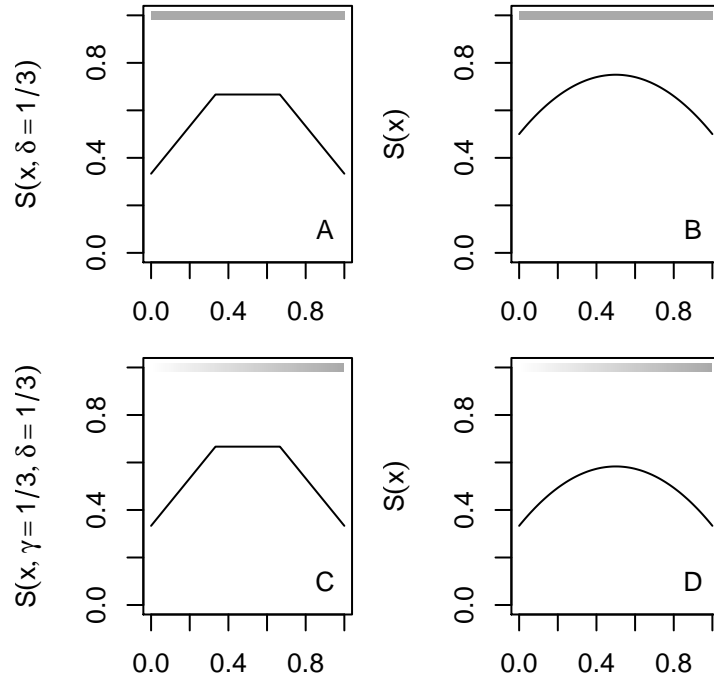


Figure 1: Species richness gradients on a line. Top row: constant environment; bottom row: monotonic environment ($g(x) = x$). Left column: $S(x; \delta, \gamma)$ for a given environmental tolerance γ and distance limit δ . Right column: $S(x)$, assuming that δ and γ are independently and uniformly distributed on $[0, 1]$. Grayscale bars at the top of each panel depict the environmental gradient, with different shades of gray corresponding to different environments.

If species vary in their distance constraints or their environmental tolerances, we can find $S(x)$
 254 by integrating $S_0(x; \gamma, \delta)$ over the distributions of γ and δ :

$$S(x) = \iint S(x; \gamma, \delta) f(\gamma) f(\delta) d\delta d\gamma \quad (3)$$

For either the constant environment or the unidirectional environment $g(x) = x$, the integral above
 256 has a simple analytical solution if δ , γ , and range origins are all independently and uniformly
 distributed on $[0, 1]$. For the constant environment, we obtain

$$S(x) = 1/2 + x(1 - x)$$

258 (Fig. 1b). For the environment $g(x) = x$, we obtain

$$S(x) = 1/3 + x(1 - x)$$

(Fig. 1d). These reproduce the symmetric, concave-down relationship that is characteristic of the
 260 MDE (Willig & Lyons, 1998; Lees *et al.*, 1999).

Now consider the reflected environment, that is, the line on $x \in [-1, 1]$, where $g(x) = |x|$. With
 262 a reflected environment, it is helpful to separate $S(x)$ into two parts. Let $S_0(x)$ be the species
 richness at x resulting from ranges originating on the same side of the reflection point as x . In
 264 contrast, let $S_1(x)$ be the species richness at x resulting from ranges originating on the opposite
 side of the reflection point. Thus, $S(x) = S_0(x) + S_1(x)$.

266 For a given γ and δ , $S_0(x; \gamma, \delta)$ is just $S(x; \gamma, \delta)$ from eq. 1 above. Finding $S_1(x; \gamma, \delta)$ requires
 a bit more thought. Without loss of generality, suppose $x > 0$. For a range originating at $y < 0$,
 268 that species' range will overlap with x if and only if all three of the following conditions hold:

- (i). x is within the species' distance constraint, i.e., $d(x, y) \leq \delta$.
- 270 • (ii). The environment at x is within the species' environmental tolerance, i.e., $|g(x) - g(y)| \leq \gamma$.
- (iii). All points between x and y lie within the species' environmental tolerance. If we assume
 272 that the environmental function is strictly increasing across $x \in [0, x_{\max}]$, this is equivalent to
 requiring that the environment at the reflection point ($g(0)$) is within the species tolerance:
 274 $|g(0) - g(y)| \leq \gamma$.

In the case that $d(x, y) = |x - y|$ and $g(x)$ satisfies conditions (E1)–(E5), then (after some algebra)
 276 it can be shown that these conditions are equivalent to

$$-g^{-1}(\gamma) \vee (x - \delta) \leq y \leq -g^{-1}(0 \vee (g(x) - \gamma)).$$

We write the left-hand side of the equation above as

$$U_1(x) = -g^{-1}(\gamma) \vee (x - \delta)$$

278 and the right-hand side as

$$L_1(x) = -g^{-1}(0 \vee (g(x) - \gamma))$$

We define the above so that L_1 represents the range origin closest to the reflection point that will support a range that overlaps x , and U_1 represents the range origin furthest from the reflection point that will support a range that overlaps x . Note that it is not guaranteed that we will have $U_1(x) < L_1(x)$; when $U_1(x) \geq L_1(x)$, then there is no spillover, and $S_1(x; \gamma, \delta) = 0$. In the special case when $g(x) = |x|$, then $U_1(x)$ simplifies to $-\gamma \vee (x - \delta)$, and $L_1(x)$ simplifies to $0 \wedge (\gamma - x)$.

284 Thus,

$$S_1(x; \gamma, \delta) = \begin{cases} \int_{U_1(x)}^{L_1(x)} f(y) dy & \text{if } U_1(x) < L_1(x) \\ 0 & \text{otherwise.} \end{cases} \quad (4)$$

(When $x = 0$, we have $S_0(x = 0; \gamma, \delta) = S_1(x = 0; \gamma, \delta)$. Thus, which component we label as S_0 vs. S_1 is irrelevant.)

Figure 2a,b shows $S(x; \gamma = 1/2, \delta = 1/4)$ and $S(x; \gamma = 1/4, \delta = 1/2)$, respectively, for the environment $g(x) = |x|$ and for a uniform distribution of range origins. These two cases provide an interesting contrast. When species ranges are limited primarily by distance (that is, δ is small and γ is large), then the internal reflection point has little to no impact on species ranges, and thus $S(x)$ recapitulates the MDE (cf. Fig. 1a,c). However, species ranges are limited predominantly by environmental tolerance (γ small and δ large), then the peak of species richness occurs close to, but not at, the reflection point. We explain this phenomenon in more depth below. To find $S(x)$, we again integrate $S(x; \gamma, \delta)$ over some distribution for γ and δ :

$$S(x) = \iint S(x; \gamma, \delta) f(\gamma) f(\delta) d\delta d\gamma.$$

Figure 2c shows $S(x)$ with γ and δ independent and uniformly distributed on $[0, 1]$.

288 The obvious and key difference between $S(x)$ for the internally reflected environment vs. $S(x)$ for either the constant or unidirectional environment is that, for the internally reflected environment, the peak of species richness may not occur at the midpoint of the domain. This occurs because the environment at the reflection point is no longer a “middle” environment; indeed, it is one of the two most extreme environments. (The other environmental extreme occurs, of course, at the ends of the domain.) The reflection point can still be reached by ranges originating on either side of

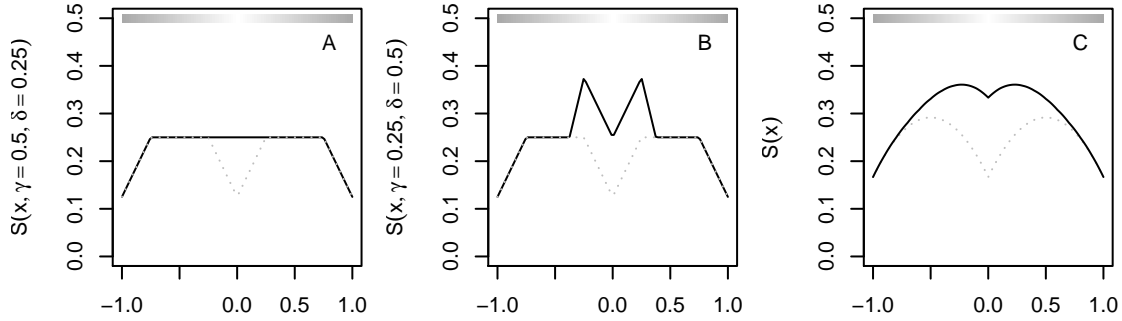


Figure 2: Species diversity gradients on an internally reflected environment with a uniform distribution of range origins. In all panels, the environment is $g(x) = |x|$. Solid lines show $S(x)$, the total species richness, and dotted lines show $S_0(x)$, the species richness resulting from species ranges with origins on the same side of the reflection point as x . The difference between the solid and dotted line gives $S_1(x)$, the species richness resulting from species ranges with origins on the opposite side of the reflection point. A: When the distance constraint predominates, species richness is constant around the reflection point, and a pattern similar to a constant or unidirectional environment appears (cf. Fig. 1a,c). B: When the environmental tolerance predominates, the peak of species richness does not occur at the midpoint of the domain. C: Species richness assuming uniform and independent distributions on δ and γ .

294 the reflection point, and thus species richness at the reflection point is greater than it is at either
of the two ends of the domain. Locations that are close to but not on the reflection point can be
296 reached by ranges originating on the same side of the reflection point, and by ranges originating on
the other side of the reflection point, as long as those species can tolerate the environment at the
298 reflection point. Put another way, species with range origins are sufficiently close to the reflection
point can have ranges that “spill over” the reflection point and thus occupy suitable habitat that is
300 available on the other side of the reflection point. Thus, species ranges pile up at a location near to,
but not exactly on, the midpoint of the domain. Figure 3 illustrates this “spillover” phenomenon.

302 The obvious motivation for a reflected gradient on Earth is a latitudinal transect that runs from
pole to pole along a meridian of longitude. With all the necessary caveats and provisos, the above
304 results appear to predict that the species richness along such a transect should not peak at the
Equator, but at low latitudes, with declines in species richness as one moves from the low-latitude
306 peak towards the Equator. To the best of our knowledge, this is the first geometric model to make
such a prediction. However, a bit of thought yields a conundrum: what if one were to consider
308 transect that starts at one point on the Equator and follows a meridian of longitude through a pole
to a second point on the Equator on the opposite side of the Earth from the first? This transect

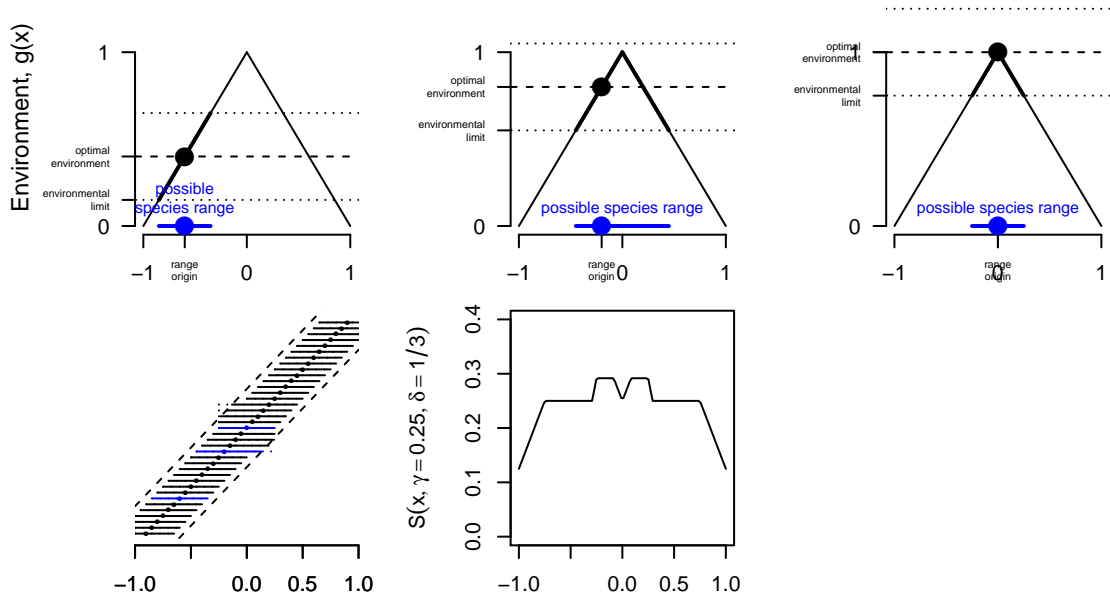


Figure 3: Range spillover leads to a peak in species richness that is offset from the reflection point on an internally reflected environment. (In this Figure, we write the environment as $g(x) = 1 - |x|$, though the same result holds for $g(x) = |x|$.) The top row shows possible species ranges for three different range origins, all with an environmental tolerance of $\gamma = 0.25$. The range originating at $x = -0.2$ (center) has the largest possible range, because it can reach the reflection point and thus “spill over” into suitable environments on the other side of the reflection point. Panels in the top row do not impose a distance constraint. Bottom left: Many different species ranges, now with a distance constraint of $\delta = 1/3$. Points show range origins, dashed diagonal lines show the distance constraint, solid horizontal lines show actual species ranges, and dotted horizontal lines (to the extent visible) show how some possible species ranges are truncated by the distance constraint. Species ranges shown in blue correspond to species origins shown in the upper panel. Bottom center: Accumulation of all species ranges to give $S(x; \gamma = 0.25, \delta = 1/3)$.

310 also has an internally reflected environment, and thus according to the results above, the peak in
species richness should occur at high latitudes close to the poles!

312 The above situation is clearly unsatisfactory. The choice of whether to run a transect from pole
to pole, or from one point on the Equator to the other on the Earth’s opposite side, is arbitrary.
314 Yet, results from the line suggest that the peak of species richness will depend on this arbitrary
choice — a conundrum that must be resolved. To do so, we extend these results to two dimensional
316 geometries such as the surface of a sphere. We will work up to the sphere by first considering a
disc and a cone, which are useful in their own right as geometric simplifications of mountains, and
318 which help build intuition about species richness in the vicinity of a pole on the sphere.

5 Results for the cone or disc

320 Consider a cone or disc with a linear environment. Under definition (D1), range origins communi-
cate on the cone or disc, and thus the bounds of integration in results for $S(x)$ can be interpreted
322 as simply the maximal extent of a range for a range originating at x .

Results for the cone follow from the observation that the cone can be ‘unrolled’. That is, imagine
324 cutting the cone along a line running from the apex to the westernmost point on the cone’s base.
The cone can then be ‘unrolled’ to form a portion of a circle with radius 1 and total area $2\pi \sin \alpha$,
326 where $\alpha \in (0, \pi/2]$ gives the opening angle of the cone. Distances on the cone correspond to simple
Euclidean distances on the unwrapped cone. On the unwrapped cone, we use the coordinate system
328 $(x, \varphi) \in [0, 1] \times [-\pi \sin \alpha, +\pi \sin \alpha]$. Here, x is the distance from the base of the cone to the apex
(so that $x = 0$ corresponds to the base, and $x = 1$ corresponds to the apex), and φ is the compass
330 direction (on the unrolled cone) with respect to “east”.

Returning to the (rolled) cone, let $S(x, \phi)$ denote the species richness at a location (x, ϕ) .
332 Because all results will be invariant to ϕ , we will simply write this as $S(x)$. As with the line,
let $S(x; \gamma, \delta)$ be the species richness found at x if all species have environmental tolerance γ and
334 distance limit δ , and let $S(x)$ indicate the species richness when either γ or δ take a non-degenerate
distribution across species. In these coordinates, a uniform distribution of range origins is given by
336 $f(x, \phi) = (1 - x)/(\pi \sin \alpha)$.

We derive $S(x; \gamma, \delta)$ first. For the moment, assume that all species have environmental tolerance
338 γ and distance limitation δ . Let $S(x, 0; \gamma, \delta)$ be the proportion of such species whose ranges overlap
the point $(x, 0)$. Consider the collection of elevations y for which a range originating at $(y, 0)$
340 will overlap $(x, 0)$. Let $L(x)$ and $U(x)$ be the smallest and largest elevations of this collection,

respectively. It turns out that $L(x)$ and $U(x)$ are exactly the same as they were for the line (eq. 2):

$$L(x) = (x - \delta) \vee g^{-1}((g(x) - \gamma) \vee 0)$$

342 and

$$U(x) = (x + \delta) \wedge g^{-1}((g(x) + \gamma) \wedge 1).$$

Now, given an elevation $y \in [L(x), U(x)]$, let $\varphi_y \in (0, \pi \sin \alpha]$ be the maximal angle (on the
 344 unrolled cone) for which a range originating at (y, φ_y) will have a range that overlaps $(x, 0)$. Using
 the law of cosines, it can be shown that φ_y is

$$\varphi_y = (\pi \sin \alpha) \wedge \cos^{-1} \left[-1 \vee \frac{(1-x)^2 + (1-y)^2 - \delta^2}{2(1-x)(1-y)} \right]. \quad (5)$$

Thus, our formula for $S(x, 0; \gamma, \delta)$ is

$$S(x, 0; \gamma, \delta) = \int_{L(x)}^{U(x)} \int_{-\varphi_y}^{\varphi_y} f(y, \varpi) d\varpi dy$$

346 Plugging in $f(y, \varpi) = (1-y)/(\pi \sin \alpha)$ gives

$$\begin{aligned} S(x, 0; \gamma, \delta) &= \int_{L(x)}^{U(x)} \int_{-\varphi_y}^{\varphi_y} \frac{(1-y)}{\pi \sin \alpha} d\varpi dy \\ &= \int_{L(x)}^{U(x)} \frac{2(1-y)\varphi_y}{\pi \sin \alpha} dy \end{aligned} \quad (6)$$

Figure 4 shows several solutions for $S(x)$ for three different values of α . One interesting aspect of
 348 this Figure is that, when the environmental constraint is more limiting than the distance constraint,
 and when the cone is not too steep (panels B and E), there is a local maximum in species richness
 350 at, but not near, the apex of the cone. This feature will re-appear when we consider LDGs in
 the neighborhood of a pole on the sphere. Note that comparisons among different values of α are
 352 complicated by the fact that the mean distance between any two randomly selected points on the
 cone shrinks as α becomes smaller (i.e., the cone becomes steeper). This suggests that to isolate
 354 the effect of the cone's steepness on species diversity gradients, the distance constraint δ should be
 scaled in accordance with α . We have yet to determine what the proper scaling relationship is, and
 356 thus one should be mindful that species ranges become larger relative to the available surface area
 of the cone as α decreases in Fig. 4.

358 If we take the cone as a first model for a mountain, it may stand to reason that environmental
 gradients will be much more important in determining species ranges than the distance limit. This
 360 suggests that it may be useful to relax the distance limit on the cone, and investigate EDGs when

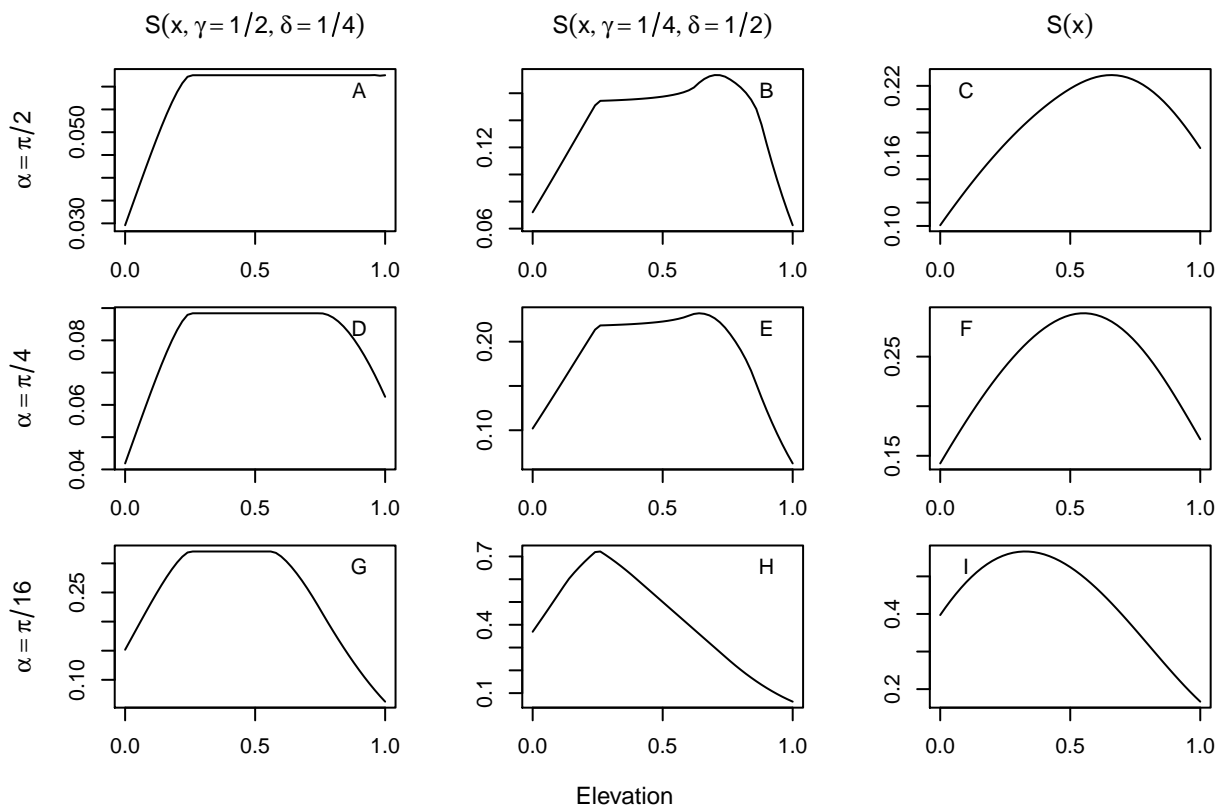


Figure 4: Species diversity gradients on a cone with a linear environment ($g(x) = x$ for $x \in [0, 1]$) and a uniform density of range origins. Top row: A flat cone (that is, a disc). Middle row: A moderately steep cone (with $\alpha = \pi/4$). Bottom row: A very steep cone ($\alpha = \pi/16$). Left column: All species are more limited by distance ($\delta = 1/4$) than by environmental tolerance ($\gamma = 1/2$). Center column: All species are more limited by environmental tolerance ($\gamma = 1/4$) than by distance constraint ($\delta = 1/2$). Note the “hump” near the peak in panels B and E. Right column: Species richness assuming uniform and independent distributions on $[0, 1]$ for δ and γ .

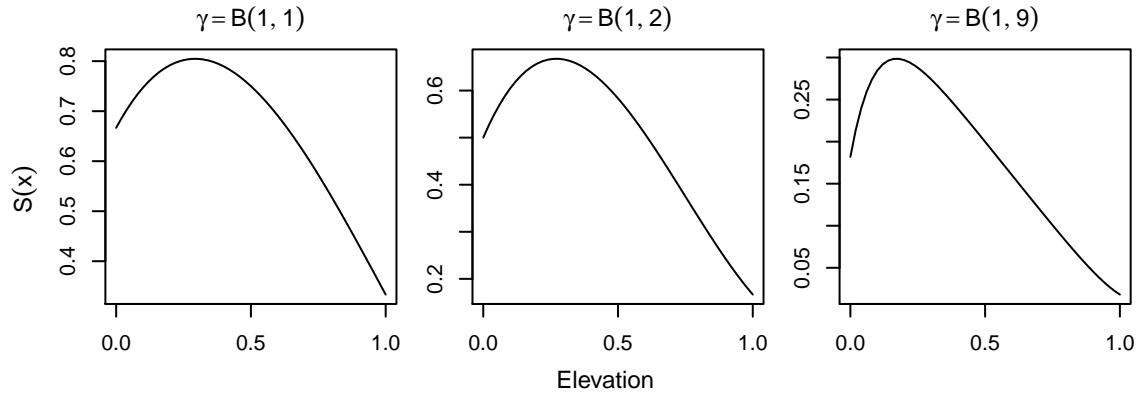


Figure 5: Species richness gradients on a cone, where the distance limit is relaxed and only the environmental tolerance limits species ranges. Environmental tolerances are uniformly distributed $[0, 1]$ (left panel), or take a Beta distribution with mean $1/3$ (center) or $1/10$ (right). When species ranges are determined exclusively by environmental tolerance, the slope of the cone (α) is irrelevant for $S(x)$.

species ranges are determined entirely by their environmental tolerance. In this situation, species
 362 ranges will wrap entirely around the cone. This scenario gives species richness gradients that peak
 closer to the base of the mountain than to its apex (Fig. 5). The exact elevation of maximal diversity
 364 depends on the distribution of γ , with smaller environmental tolerances yielding a maximum closer
 to the base of the mountain. When the distance constraint is relaxed as it is here, the slope of the
 366 cone (α) has no effect on the results.

Before moving on, we note that all of the results above are for isolated cones, in the sense that
 368 we assume the base of the cone forms a boundary between hospitable and inhospitable habitat. For
 an oceanic mountain, this may be a reasonable assumption. For a terrestrial mountain, however,
 370 one would expect that the habitat near the base of the mountain would be accessible by species
 living on the surrounding landscape. Such an argument suggests that elevational diversity gradients
 372 on terrestrial mountains should have greater species richness near the mountain's base than Figure
 5 suggests. In this scenario, the degree to which encroachment from species with range origins
 374 on the surrounding landscape alters the shape of $S(x)$ depends entirely on how species ranges
 on the surrounding landscape compare to species ranges on the mountain. If we assume that
 376 (a) the distance constraint is not relevant at the scale of a mountain, (b) the environment is
 the same everywhere on the surrounding landscape, and (c) the surrounding landscape extends
 378 indefinitely, then the species richness on the surrounding landscape will be infinite! Clearly such

logic is unsatisfactory. Therefore, for the time being, we only observe that encroachment from
 380 species on any surrounding landscape should increase species richness at low elevations relative to
 what Fig. 5 suggests.

382 6 Results for the surface of the sphere

We now turn to the surface of the sphere, a first model for species diversity gradients on Earth.
 384 We will see that, in the neighborhood of the Equator, results on the sphere echo results from the
 line segment with the reflected environment, whereas in the neighborhood of the pole, results on
 386 the sphere echo results near the peak of the cone.

Recall that our coordinate system is $x \in [-\pi/2, \pi/2]$ for latitude (with $x = -\pi/2$ corresponding
 388 to the South Pole, $x = 0$ corresponding to the Equator, and $x = \pi/2$ corresponding to the North
 Pole). For longitude, we use $\phi \in (-\pi, \pi]$. The great-circle distance between any two points on the
 390 unit sphere is given by the geodetic form of the spherical law of cosines:

$$d((x_1, \phi_1), (x_2, \phi_2)) = \cos^{-1}(\sin x_1 \sin x_2 + \cos x_1 \cos x_2 \cos(\phi_1 - \phi_2)) \quad (7)$$

As a special case of eq. 7, note that if two points share the same longitude, then $d((x, \phi), (y, \phi)) =$
 392 $|x - y|$.

Again, let $S(x)$ be the total species richness at latitude $x \in [0, \pi/2]$ (all results will be invariant
 394 with respect to longitude). Let $S_0(x)$ be the species richness resulting from ranges originating on
 the same side of the Equator as x , and let $S_1(x)$ be the species richness resulting from ranges
 396 originating on the opposite side of the Equator as x . We are most interested in the environment
 $g(x) = 1 - \cos x$, because this is a reasonable model for how solar inputs vary across the surface
 398 of the Earth. For comparison with earlier results, we will also consider the linear environment
 $g(x) = |2x/\pi|$. The surface of the sphere with either environment does not communicate because of
 400 the reflection at the Equator. Further, because this is a two-dimensional geometry, the difference
 between our definitions of species centers is again relevant, and we again adopt definition (D1) for
 402 mathematical convenience. Finally, a uniform distribution of range origins on the sphere is given
 by $f(x, \phi) = (1/4\pi)^{-1} \cos x$.

404 We can derive $S_0(x, 0; \gamma, \delta)$ using a logic similar to that used for the cone / disc. Our solution
 will take the form

$$S_0(x, 0; \gamma, \delta) = \int_{L(x)}^{U(x)} \int_{-\phi_y}^{\phi_y} f(y, \varphi) d\varphi dy.$$

406 $L(x)$ and $U(x)$ are identical to the cone / disc, or to the line, that is,

$$L(x) = (x - \delta) \vee g^{-1}((g(x) - \gamma) \vee 0)$$

and

$$U(x) = (x + \delta) \wedge g^{-1}((g(x) + \gamma) \wedge 1).$$

408 Given a latitude $y \in [L(x), U(x)]$, $\phi_y \in (0, \pi]$ is the maximal longitude for which a range originating at (y, ϕ_y) will overlap $(x, 0)$. To find ϕ_y we apply the distance formula in eq. 7:

$$\begin{aligned} d((x, 0), (y, \phi_y)) &= \delta \\ \Rightarrow \phi_y &= \cos^{-1} \left[-1 \vee \frac{\cos \delta - \sin x \sin y}{\cos x \cos y} \right] \end{aligned} \quad (8)$$

410 where the quantity in square brackets evaluates to -1 (and thus $\phi_y = \pi$) if the entire parallel at y is within a distance δ of $(x, 0)$. Plugging in gives

$$\begin{aligned} S_0(x, 0; \gamma, \delta) &= \int_{L(x)}^{U(x)} \int_{-\phi_y}^{\phi_y} f(y, \varphi) d\varphi dy \\ &= \int_{L(x)}^{U(x)} \int_{-\phi_y}^{\phi_y} \cos y (4\pi)^{-1} d\varphi dy \\ &= \int_{L(x)}^{U(x)} (2\pi)^{-1} \cos y \phi_y dy \\ &= \int_{L(x)}^{U(x)} (2\pi)^{-1} \cos y \cos^{-1} \left[-1 \vee \frac{\cos \delta - \sin x \sin y}{\cos x \cos y} \right] dy. \end{aligned} \quad (9)$$

412 $S_1(x; \gamma, \delta)$ follows similarly, again using a logic similar to eq. 4. First, we only have $S_1(x; \gamma, \delta) > 0$ if $-g^{-1}(\gamma) \vee (x - \delta) \leq -g^{-1}(0 \vee (g(x) - \gamma))$ (otherwise $S_1(x; \gamma, \delta) = 0$). As with the line, write
414 $U_1(x) = -g^{-1}(\gamma) \vee (x - \delta)$, and write $L_1(x) = -g^{-1}(0 \vee (g(x) - \gamma))$. Then, if $U_1(x) < L_1(x)$

$$\begin{aligned} S_1(x; \gamma, \delta) &= \int_{-U_1(x)}^{-L_1(x)} \int_{-\phi_y}^{\phi_y} f(y, \varphi) d\varphi dy \\ &= \int_{-U_1(x)}^{-L_1(x)} (2\pi)^{-1} \cos y \cos^{-1} \left[-1 \vee \frac{\cos \delta - \sin x \sin y}{\cos x \cos y} \right] dy. \end{aligned} \quad (10)$$

Figure 6 shows $S(x; \gamma, \delta)$ for several choices of γ and δ , and shows $S(x)$ when γ and δ are
416 independent and uniformly distributed on $[0, 1]$ and $[0, \pi/2]$, respectively. The most important panel of Fig. 6 is panel (h), which shows the expected species richness for a cosine environment
418 and with γ and δ independently and uniformly distributed on their allowable ranges. This plot shows a broad region of flat species richness near the equator, followed by a steep drop-off in species
420 richness at high latitudes.

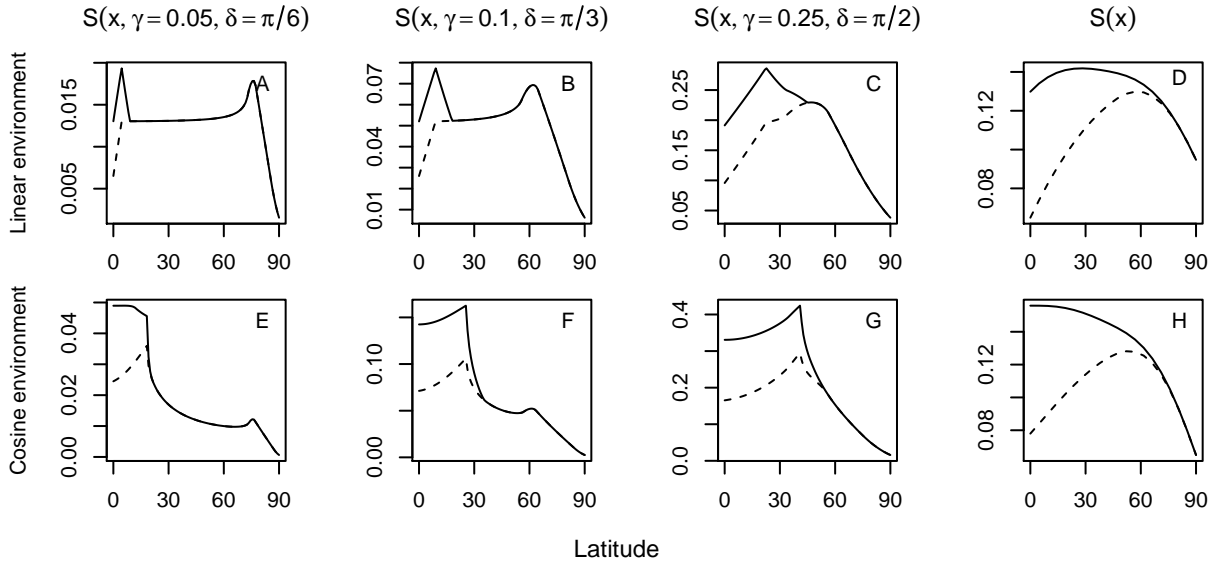


Figure 6: Species richness gradients on a latitudinal transect on the surface of a sphere, for various combinations of γ and δ . Top row: linear environment ($g(x) = |2\pi/x|$). Bottom row: cosine environment ($g(x) = 1 - \cos x$). Left three columns: γ and δ fixed at specific values. Right column: γ and δ are independent and uniformly distributed on $[0, 1]$ and $[0, \pi/2]$, respectively. Dotted lines show $S_0(x)$, the species richness resulting from ranges with origins on the same side of the Equator as x .

Figure 7 shows $S(x)$ for various distributions of γ and δ . For both parameters, we use Beta
422 distributions with the first shape parameter (commonly written as α) set equal to 1, and allow the
second shape parameter (commonly β) to be ≥ 1 . (In the case of δ , we set $\delta = \delta_{\max}B$, where B is a
424 Beta-distributed random variate, and $\delta_{\max} = \pi/2$ is the maximum value of δ that we allow.) When
 $\beta = 1$, this gives uniform distributions. When $\beta > 1$, the distribution becomes more aggregated at
426 small values, with the density having a mode at 0 and declining monotonically as the parameter
increases. The mean value of the Beta distribution is $1/(1 + \beta)$. The left-most column of figure
428 7 holds δ fixed at π , so that species ranges are determined exclusively by their environmental
tolerance. The right-most three columns of Figure 7 show independent distributions for both γ and
430 δ .

Figure 7 shows the model is capable of producing a rich variety of latitudinal gradients in
432 species diversity, depending on the assumptions made about the distributions of γ and δ . Despite
this variety, many combinations of γ and δ predict that species richness will be reasonably constant
434 at low latitudes, and in many cases species diversity will actually increase subtly as one moves
away from the Equator. To the best of our knowledge, this model is the first geometric model to

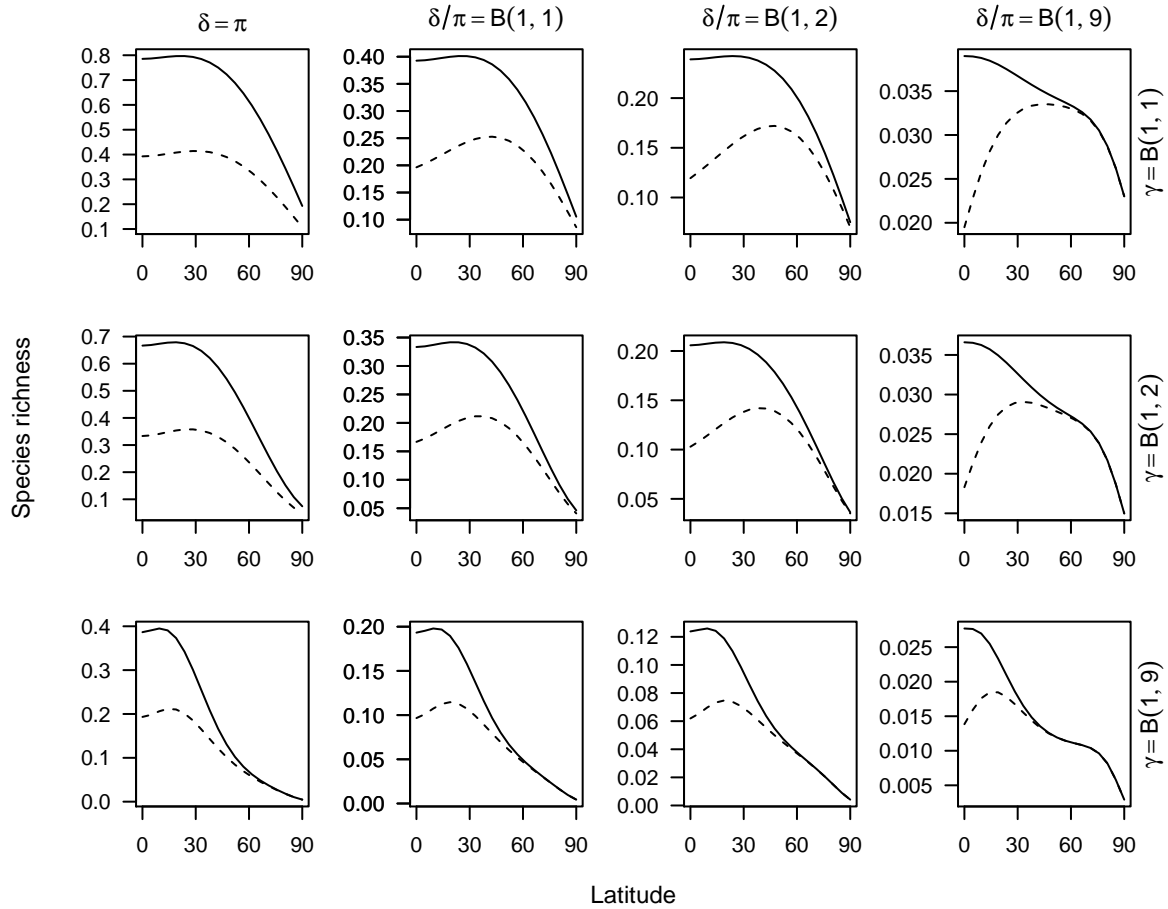


Figure 7: Species richness gradients on a latitudinal transect on the surface of a sphere, for various distributions for γ and δ . Left column shows $\delta = \pi$ for all species, which effectively removes the distance constraint so that only the environmental tolerance dictates species ranges. For all other columns, the distribution on δ becomes more concentrated on smaller values going from left to right. Rows show different distributions for γ , where the distribution on γ becomes more concentrated on smaller values going from top to bottom. Dotted lines show $S_0(x)$, the species richness resulting from ranges with origins on the same side of the Equator as x .

436 make this prediction. The region of relatively constant species richness at low latitudes is followed
 by a sharp drop in species diversity at intermediate latitudes. This region of rapidly declining
 438 species diversity is found at (relatively) lower latitudes when species can only tolerate a narrow
 range of environments, and occurs at higher latitudes when species can tolerate a broader range
 440 of environments. Under some scenarios (especially when the distance limitation is small), there is
 a zone at high latitudes where the loss in species diversity slows, before dropping precipitously as
 442 one approaches the pole. This second shoulder in the species distribution curve at high latitudes
 is also a feature that, to the best of our knowledge, our model is the first to predict.

444 7 Ice caps

Finally, we consider the impact of an ice cap (or zone that does not allow life) on the peak of a
 446 cone or at the poles of a sphere. Incorporating an ice cap is straightforward. On a cone, we simply
 have to adjust $U(x)$ in eq. 2 to:

$$U(x) = [(x + \delta) \wedge g^{-1}((g(x) + \gamma) \wedge 1)] \wedge \tilde{x} \quad (11)$$

448 We define $S(x) = 0$ when $x > \tilde{x}$. For the sphere, ice caps enter in at the poles, and so we adjust
 $U(x)$ as in eq. 11, and we adjust $-U_1(x)$ to be

$$U_1(x) = [-g^{-1}(\gamma) \vee (x - \delta)] \vee -\tilde{x}.$$

450 Figure 8 shows that ice caps compress $S(x)$, but otherwise have little effect on the shape of $S(x)$
 vs. x . Importantly, the presence of ice caps does not alter the major qualitative features of $S(x)$
 452 that we have noted here, including the low-elevation peak of species richness on conical mountains,
 the flat or gradually increasing species diversity at low latitudes on the sphere, and (under some
 454 conditions) the presence of a high-latitude shoulder in species diversity on the sphere.

8 Summary and Discussion

456 The model presented here shows that the interplay among the geometry of the environment, niche
 fidelity and dispersal limitation can yield a surprisingly rich variety of latitudinal and elevational
 458 gradients in biological diversity. This “environmental geometry” model predicts qualitative struc-
 ture to diversity gradients that is more nuanced than previous geometric models have suggested
 460 (e.g. Colwell & Hurtt, 1994; Lees *et al.*, 1999; Gorelick, 2008). Understanding the mechanisms
 behind these structures sharpens our understanding of how environmental geometry may influence

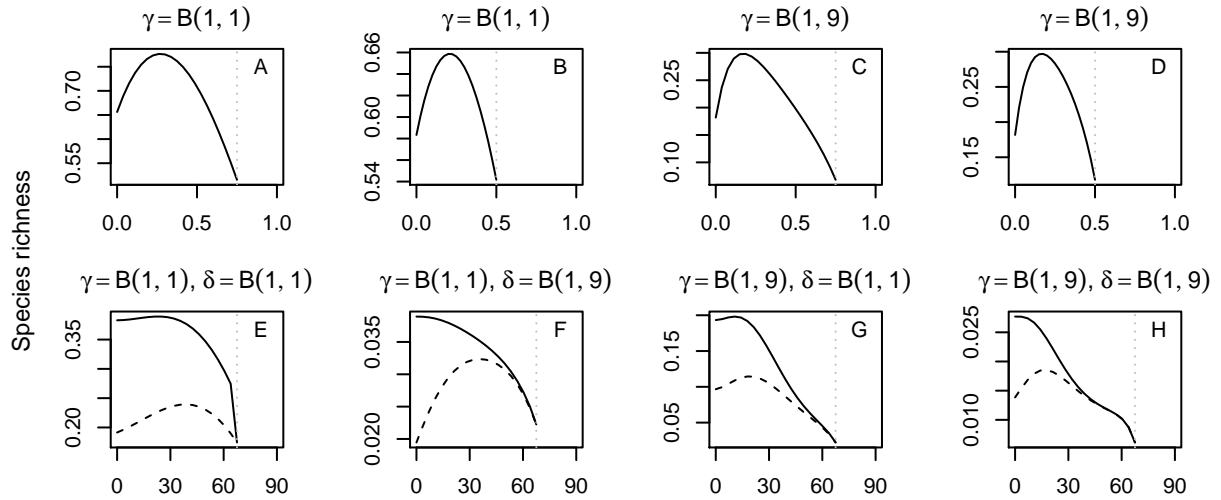


Figure 8: Diversity gradients on cones and spheres with icecaps. Throughout, the position of the icecap is shown with a dotted vertical line. Top row: Elevational diversity gradients on a cone (actually a disc) when species ranges are determined only by their environmental tolerance. Left two panels: γ is distributed uniformly on $[0, 1]$; right two panels: γ is concentrated at small environmental tolerances. Bottom row: Latitudinal diversity gradients on the sphere for various distributions of γ and δ . In panels E–H, ice caps extend to $x = 3\pi/8$, or 67.5° latitude, which loosely coincides with the position of the Arctic and Antarctic circles on Earth.

462 diversity gradients, and how these effects are modulated by the ecological properties of the taxa
considered. These insights improve our ability to resolve the impacts of the many drivers that
464 combine to generate the diversity gradients that typify life (Colwell, 2011).

On a sphere, this model predicts latitudinal diversity gradients (LDGs) with more complex
466 structure than the quasi-parabolic relationship between latitude and species richness predicted
by most other geometric models (e.g., Colwell & Hurtt, 1994; Lees *et al.*, 1999; Gorelick, 2008)).
468 Prominent features of this structure include broad plateaus in diversity at low latitudes, especially
when species ranges are large; subtle Equatorial valleys in species richness when dispersal limitation
470 is weak and environmental niches are narrow; rapid declines in biological diversity at the low-to-
mid latitude “shoulders” of the low-latitude plateau; and occasional secondary plateaus in species
472 richness at mid-to-high latitudes, especially when environmental niches are narrow and dispersal
limitation is strong. Although a formal confrontation with data awaits future work, the concordance
474 between several of these predictions and documented LDGs is striking. In the most recent edition
of their text, Lomolino *et al.* (2010, p. 670) observed that “rather than exhibiting a continuous
476 decline in species density from the Equator to the poles, most taxa exhibit a pattern of relatively
high, albeit variable, diversity in the tropics marked by a rapid decline through the subtropics and
478 much more modest declines through the higher latitudes.” This statement matches the qualitative
predictions of our model nearly to a tee, and suggests limits to environmental niches and range
480 sizes on the stronger side of those that we have explored here (Fig. 7).

Some of the more surprising predictions of this model for LDGs are occasional Equatorial
482 diversity valleys and high-latitude diversity plateaus (or even secondary peaks; Fig. 6). Equatorial
valleys in species diversity are well documented for oceanic taxa. For example, Tittensor *et al.*
484 (2010) observed that most oceanic taxa peak in richness between 20°–40° latitude, while Rutherford
et al. (1999) and Yasuhara *et al.* (2012) have shown that planktic foraminiferan diversity gradually
486 increases from the Equator to the subtropics before declining sharply beyond $\sim 30^\circ$. The match
with oceanic data is compelling, as the simplified setting used in this model would seem to more
488 closely resemble oceanic conditions than terrestrial ones, where a variety of other important factors
such as continental boundaries and precipitation gradients surely participate in LDGs. Empirical
490 evidence for a secondary polar plateau in species richness is harder to find. Roy *et al.* (1998) found
a secondary peak in marine copepod diversity between 50° – 60° N in the eastern Pacific, although
492 they speculated that this was “at least partly an artifact” of the particular geography of the Gulf
of Alaska and the Bering Sea. Because the high-latitude plateau is driven by species ranges that

494 partially encircle a pole, the plateau would be more likely to occur in the Southern ocean, if it
occurs at all.

496 On a cone, our model predicts a unimodal, “hump-shaped” relationship between species richness
and elevation, with a peak in richness closer to the base of the cone than its apex. While many
498 have observed that a hump-shaped relationship between species richness and elevation is common
(e.g. Rahbek, 1995; Lomolino, 2001), few have commented on the precise location of the diversity
500 peak. Our informal survey of the literature suggests that low-elevation peaks in species richness
are common, and can be found for such taxa as birds (Terborgh, 1977), rodents (Rahbek, 1995),
502 ants (Bishop *et al.*, 2014), ferns (Bhattarai *et al.*, 2004), and fungi (Miyamoto *et al.*, 2014). If this
pattern withstands deeper scrutiny, our model provides one mechanism that could explain it.

504 To sum up, while environmental geometry is unlikely to be the sole driver of diversity gradients,
the results here suggest that the even simple geometries can generate surprisingly nuanced gradients
506 in species richness when combined with basic ecological limits on species ranges. Although our
casual comparison of model predictions with data is far from rigorous, the striking concordance
508 between model predictions and prevailing empirical patterns suggests that the role of geometry may
be deeper and more pervasive than previously appreciated. The success of this model in capturing
510 the basic features of many LDGs and EDGs also suggests that it could be profitably adapted to
less conventional diversity gradients along more complex geometries. Other interesting settings to
512 explore may include the microbiome of the human skin (Costello *et al.*, 2012) or gastrointestinal
tract (Stearns *et al.*, 2011), bathymetric (depth) gradients in the ocean (Pineda & Caswell, 1998),
514 or even the hypothetical species richness gradients on candidate planets for extraterrestrial life
(Snyder-Beattie, 2013).

516 9 Acknowledgments

This work was supported by NSF awards 08-42101, 10-15825 and 12-41794 to KG.

518 References

- Bhattarai, K. R., Vetaas, O. R. & Grytnes, J. A. (2004). Fern species richness along a central
520 Himalayan elevational gradient, Nepal. *Journal of Biogeography*, 31, 389–400.
- Bishop, T. R., Robertson, M. P., Rensburg, B. J. & Parr, C. L. (2014). Elevation–diversity patterns
522 through space and time: ant communities of the Maloti-Drakensberg mountains of southern
Africa. *Journal of Biogeography*, 41, 2256–2268.
- 524 Brown, J. H. (2014). Why are there so many species in the tropics? *Journal of Biogeography*, 41,
8–22.

- 526 Colwell, R. K. (2011). Biogeographical gradient theory. In: *The theory of ecology* (eds. Scheiner, S. M. & Willig, M. R.). University of Chicago Press, pp. 309–330.
- 528 Colwell, R. K., Gotelli, N. J., Rahbek, C., Entsminger, G. L., Farrell, C. & Graves, G. R. (2009).
530 Peaks, plateaus, canyons, and craters: the complex geometry of simple mid-domain effect models.
Evolutionary Ecology Research, 11, 355–370.
- Colwell, R. K. & Hurtt, G. C. (1994). Nonbiological gradients in species richness and a spurious
532 Rapoport effect. *The American Naturalist*, 144, 570–595.
- Colwell, R. K. & Lees, D. C. (2000). The mid-domain effect: geometric constraints on the geography
534 of species richness. *Trends in Ecology & Evolution*, 15, 70–76.
- Connolly, S. R. (2005). Process-based models of species distributions and the mid-domain effect.
536 *The American Naturalist*, 166, 1–11.
- Costello, E. K., Stagaman, K., Dethlefsen, L., Bohannan, B. J. & Relman, D. A. (2012). The
538 application of ecological theory toward an understanding of the human microbiome. *Science*,
336, 1255–1262.
- 540 Crame, J. A. (2001). Taxonomic diversity gradients through geological time. *Diversity and Distri-*
butions, 7, 175–189.
- 542 Davies, R. G., Orme, C. D. L., Storch, D., Olson, V. A., Thomas, G. H., Ross, S. G., Ding, T.-S.,
544 Rasmussen, P. C., Bennett, P. M., Owens, I. P. *et al.* (2007). Topography, energy and the global
distribution of bird species richness. *Proceedings of the Royal Society B: Biological Sciences*, 274,
1189–1197.
- 546 Gorelick, R. (2008). Species richness and the analytic geometry of latitudinal and altitudinal
gradients. *Acta Biotheoretica*, 56, 197–203.
- 548 Hillebrand, H. (2004). On the generality of the latitudinal diversity gradient. *The American*
Naturalist, 163, 192–211.
- 550 Jablonski, D., Roy, K. & Valentine, J. W. (2006). Out of the tropics: evolutionary dynamics of the
latitudinal diversity gradient. *Science*, 314, 102–106.
- 552 Jetz, W. & Rahbek, C. (2001). Geometric constraints explain much of the species richness pattern
in African birds. *Proceedings of the National Academy of Sciences*, 98, 5661–5666.
- 554 Lees, D. C., Kremen, C. & Andriamampianina, L. (1999). A null model for species richness
gradients: bounded range overlap of butterflies and other rainforest endemics in Madagascar.
556 *Biological Journal of the Linnean Society*, 67, 529–584.
- Lomolino, M. (2001). Elevation gradients of species-density: historical and prospective views.
558 *Global Ecology and Biogeography*, 10, 3–13.
- Lomolino, M. V., Riddle, B. R., Whittaker, R. J. & Brown, J. H. (2010). *Biogeography*. 4th edn.
560 Sinauer Associates Sunderland, MA.
- Mittelbach, G. G., Schemske, D. W., Cornell, H. V., Allen, A. P., Brown, J. M., Bush, M. B.,
562 Harrison, S. P., Hurlbert, A. H., Knowlton, N., Lessios, H. A. *et al.* (2007). Evolution and
the latitudinal diversity gradient: speciation, extinction and biogeography. *Ecology Letters*, 10,
564 315–331.
- Miyamoto, Y., Nakano, T., Hattori, M. & Nara, K. (2014). The mid-domain effect in ectomycor-
566 rhizal fungi: range overlap along an elevation gradient on Mount Fuji, Japan. *ISME Journal*, 8,
1739–1746.

- 568 Pineda, J. & Caswell, H. (1998). Bathymetric species-diversity patterns and boundary constraints
on vertical range distributions. *Deep Sea Research Part II: Topical Studies in Oceanography*, 45,
570 83–101.
- Rahbek, C. (1995). The elevational gradient of species richness: a uniform pattern? *Ecography*,
572 18, 200–205.
- Rangel, T. F. L. & Diniz-Filho, J. A. F. (2005). An evolutionary tolerance model explaining spatial
574 patterns in species richness under environmental gradients and geometric constraints. *Ecography*,
28, 253–263.
- 576 Rangel, T. F. L., Diniz-Filho, J. A. F. & Colwell, R. K. (2007). Species richness and evolutionary
niche dynamics: a spatial pattern-oriented simulation experiment. *The American Naturalist*,
578 170, 602–616.
- Rosenzweig, M. L. (1995). *Species diversity in space and time*. Cambridge University Press.
- 580 Roy, K., Jablonski, D., Valentine, J. W. & Rosenberg, G. (1998). Marine latitudinal diversity
gradients: tests of causal hypotheses. *Proceedings of the National Academy of Sciences*, 95,
582 3699–3702.
- Rutherford, S., D’Hondt, S. & Prell, W. (1999). Environmental controls on the geographic distri-
584 bution of zooplankton diversity. *Nature*, 400, 749–753.
- Snyder-Beattie, A. E. (2013). *New models for latitudinal biodiversity gradients and implications in
our search for extraterrestrial life*. Master’s thesis, North Carolina State University.
- 588 Stearns, J. C., Lynch, M. D., Senadheera, D. B., Tenenbaum, H. C., Goldberg, M. B., Cvitkovitch,
D. G., Croitoru, K., Moreno-Hagelsieb, G. & Neufeld, J. D. (2011). Bacterial biogeography of
the human digestive tract. *Scientific reports*, 1.
- 590 Terborgh, J. (1973). On the notion of favorableness in plant ecology. *The American Naturalist*,
107, 481–501.
- 592 Terborgh, J. (1977). Bird species diversity on an Andean elevational gradient. *Ecology*, 58, 1007–
1019.
- 594 Tittensor, D. P., Mora, C., Jetz, W., Lotze, H. K., Ricard, D., Berghe, E. V. & Worm, B. (2010).
Global patterns and predictors of marine biodiversity across taxa. *Nature*, 466, 1098–1101.
- 596 Willig, M. R., Kaufman, D. M. & Stevens, R. D. (2003). Latitudinal gradients of biodiversity:
pattern, process, scale, and synthesis. *Annual Review of Ecology, Evolution, and Systematics*,
598 34, 273–309.
- Willig, M. R. & Lyons, S. K. (1998). An analytical model of latitudinal gradients of species richness
600 with an empirical test for marsupials and bats in the New World. *Oikos*, 81, 93–98.
- 602 Yasuhara, M., Hunt, G., Dowsett, H. J., Robinson, M. M. & Stoll, D. K. (2012). Latitudinal
species diversity gradient of marine zooplankton for the last three million years. *Ecology Letters*,
15, 1174–1179.